A ES
ISSN: 2096-3246
Volume 58, Issue 01, 2026

PHYTO-ENGINEERED CUBIMETALLIC NANOSTRUCTURES DERIVED FROM CARALLUMA STALAGMIFERA: MULTIMODAL SPECTROSCOPIC–MORPHOLOGICAL INSIGHTS AND FUNCTIONAL PERFORMANCE EVALUATION

Ramarao Gollapalli[1], Aele Manohar[1], K. Suresh Babu[1]
[1]Faculty of Pharmacy, Lincoln University College, Malaysia.
ramagollapalli80@gmail.com, aelemanohar@gmail.com, babuiict@gmail.com

Abstract
The growing demand for eco-friendly multifunctional nanomaterials has stimulated extensive research on sustainable synthesis approaches using plant-based resources. In this context, green synthesis has emerged as an effective alternative to conventional chemical methods due to its low toxicity, cost effectiveness, and environmental compatibility. The present study reports the phyto-mediated synthesis of functional multimetallic nanostructures using *Caralluma stalagmifera* extract as a natural reducing and stabilizing agent. The synthesized nanomaterial was characterized for studying its various physical, optical, morphological, compositional, and biological properties. The results of x-ray diffraction analysis revealed that the obtained nanomaterial was crystalline in nature and showed successful formation of its phases. FTIR results revealed the presence of functional groups responsible for nanoparticle reduction and stabilization, while UV–Visible spectroscopy demonstrated favorable optical absorption characteristics with semiconducting behavior. Raman spectroscopy further verified vibrational features and structural quality of the material. Surface morphology investigated through SEM showed irregularly distributed nanoscale grains with partial agglomeration, and EDX analysis confirmed the presence of major constituent elements including O, Na, Cl, K, Co, and Ag. Dielectric studies indicated frequency-dependent electrical behavior with promising dielectric constant and loss characteristics suitable for electronic applications. In addition, antimicrobial and antifungal investigations demonstrated effective inhibition against selected pathogenic microorganisms, confirming the biological potential of the synthesized samples. The integrated results establish a clear relationship between composition, structure, and multifunctional performance. Overall, this study highlights the capability of *Caralluma stalagmifera* mediated green synthesis for producing advanced nanomaterials with potential applications in biomedical coatings, sensors, environmental remediation, dielectric devices, and other emerging technologies.

Keywords: Antifungal, Antimicrobial, Dielectric, Nanomaterial, bimetallic nanostructures

1. Introduction

Nanostructured materials possess much more significance than bulk material due to their unique optical, electrical, structural, and biological behavior compared to bulk materials [1]. Nanostructured metal oxides and nanocomposites find much use as sensors, photodegradation reactions, anti-bacterial coatings, dielectric material, optoelectronics, and energy storage due to their higher surface-to-volume ratio, controllable band gap, increased electron mobility, and enhanced surface activity [2]. The physiochemical properties of nanomaterials depend heavily on synthesis method, particle size, shape, crystallinity, and elemental composition [3]. Thus, comprehensive characterization by analytical methods like X-ray diffraction (XRD), Fourier transform infrared spectroscopy (FTIR),

UV-Visible spectroscopy, Raman spectroscopy, scanning electron microscopy (SEM), energy dispersive X-ray spectroscopy (EDX), and dielectric analysis is crucial for comprehending their functional capabilities [4]. Moreover, rising environmental consciousness and need for multifunctional materials have inspired the innovation of new nanostructures with both structural stability and biological activity, especially the antimicrobial resistance to pathogenic microbes [5].

Existing studies have successfully synthesized various nanomaterials using chemical precipitation, sol-gel, hydrothermal, combustion, and green chemistry approaches to increase the functionality of the resulting products [6]. Past research studies showed that the synthesis process plays a significant role in enhancing the crystallinity, optical absorption, dielectric constant, and antibacterial activity [7]. However, past research studies only focused on the structural and optical characteristics of the synthesized nanomaterials without developing a link between the morphology, composition, and multifunctional characteristics of the material [8]. Particle agglomeration, impurities in phases, irregularity in the growth of grains, and lack of surface homogeneity hinder the efficient utilization of the fabricated nanomaterials [9]. The distribution of elements and defect states has not been adequately analyzed, limiting knowledge about charge transfer and dielectric response. Some researchers have also reported antimicrobial effectiveness without linking the results with surface morphology at the nanoscale level. Comparison of the dielectric, optical, and biological attributes of a material system has not been done.

The proposed research work attempts to conduct a effective study and systematic analysis of the performance of an efficient nanomaterial with advanced features including structural, optical, dielectric, and antimicrobial properties [10]. This can be done by analyzing the sample prepared using XRD for crystalline phase identification and lattice nature analysis, FTIR, and Raman spectroscopy techniques for chemical bond confirmation and vibration studies respectively. Further, the optical absorption behavior and band gap energy estimation can be conducted via UV–VI spectroscopy analysis to analyze its importance in photocatalysis and photonic devices. SEM technique would help understand the morphology, arrangement of grains, and particle distribution on the surface of the sample, while elemental analysis would be determined through EDX method. Dielectric studies would enable to study frequency dependent polarization behavior and electrical analysis of the sample. Also, the biological applications of the developed nanomaterial would be studied through antimicrobial and antifungal tests.

1.1 Research Significance

The significance of the research work is associated with the creation of a nanomaterial that could be used as an advanced one in terms of structural, optical, dielectric, and antibacterial properties. This research work has made it possible to gain a much better understanding of the relationship between various factors of synthesis, materials, and their properties due to advanced testing methods.

1.2 Research Motivation

The growing demand for multifunctional materials with improved electrical, optical, and biological capabilities is the main motivation of this study. Current limitations posed by the unstable, ineffective, and non-antimicrobial capabilities of materials available compel researchers to

investigate into this field. Tailoring the material capabilities using synthesis and characterization processes has been a key driving factor of research.

1.3 Research Objectives

1. To synthesize a functional nanomaterial with improved structural and surface properties.
2. To characterize the prepared material using XRD, FTIR, UV–Vis, Raman, SEM, and EDX techniques.
3. To evaluate the dielectric, optical, antimicrobial, and antifungal performance of the synthesized sample.
4. To establish the relationship between material structure, composition, and functional properties for practical applications.

1.4 Key Contributions

1. Developed a functional nanomaterial with enhanced structural and surface characteristics through an effective synthesis process.
2. Performed comprehensive material characterization using XRD, FTIR, UV–Vis, Raman, SEM, and EDX techniques.
3. Demonstrated improved dielectric, optical, antimicrobial, and antifungal properties of the synthesized sample.
4. Established a clear relationship between structure, composition, and multifunctional performance for practical applications.

1.5 Rest of the Section

The rest of the section is organized as follows. Section 2 Presents the Literature Review, Section 3 describes the experimental characterization techniques, including XRD, FTIR, UV–Vis, Raman, SEM, EDX, and dielectric analysis. Section 4 discusses the obtained results related to structural, optical, electrical, antimicrobial, and antifungal properties. Finally, Section 5 concludes the study with key findings and future research directions.

2. Literature review

Pratap et al. [11] investigated the nanocomposites of ZnO-MWCNTs obtained via an economical sol-gel method in order to enhance their structure and dielectric properties for applications in energy storage. Pure ZnO and samples of ZnO-MWCNTs containing 5 wt.% and 10 wt.% MWCNTs were produced, analyzed by XRD, Raman spectroscopy, TEM, SAED, and dielectric property analysis. The findings indicated that with an increase in the weight percentage of MWCNTs, there was enhancement in peak broadening, the value of ID/IG ratio, dielectric constant, reduction in loss, and AC conductivity.

Kumari et al. [12] developed nanoscale structures of zinc-doped nickel chromites by a low-temperature citrate gel method for improving multifunctional behavior. Various compositions with different Zn concentrations were fabricated and studied by using XRD, FESEM, EDS, dielectric, antibacterial, and magnetic techniques. Single-phase FCC structure of 9-20 nm grain size along with enhanced bioactivity and reduced magnetic coercivity were observed with increased amounts of Zn. Comparison study showed that $ZnCr_2O_4$ had superior performance among all other compounds. But further work is needed in biocompatibility and applicability aspects.

Awad et al. [13] explores the superior electrochemical and dielectric properties of nanomaterials. The research uses a sustainable solvothermal approach that employs the extraction of Trigonella foenum-graecum seeds to synthesize nanowires with better performance. The findings confirm that the fabricated material exhibits structural soundness and incorporates Ag ions through the XRD, SEM, FTIR, EDS, and XPS techniques. The experiment reports a lower bandgap value of 2.78 eV and higher capacitance of 0.966 F/g.

Ekwujuru et al. [14] investigates the antimicrobial agents to overcome the resistance developed to antibiotics. In this study, CdS nanoparticles were prepared and characterized through the techniques of structure and spectroscopy. Methods utilized for assessment were MIC, MBC, and diffusion in an agar plate experiment against Escherichia coli and Staphylococcus aureus. High effectiveness against E. coli was noted and exhibited dependence on concentration and temperature. Nonetheless, toxicity makes biomedical uses difficult.

Zulfiqar et al. [15] investigates the utilization of green synthesis approaches to develop Eucalyptus globulus extract-based nanoparticles for the photodegradation process of antibiotics. Eco-friendly synthesis techniques to produce nanoparticles, biochar, and nanocomposites for higher catalytic activity have been suggested in this paper. The experimentation involves the degradation of Ciprofloxacin and Amoxicillin through optimized parameters of pH, concentration, and irradiation. The nanocomposites were found to be more efficient according to pseudo-first-order kinetics.

Raza et al. [16] investigates the use of supercapacitors made from the Sansevieria trifasciata plant extract. The green synthesis process used in making the ZnO nanoparticles and Ag@ZnO nanocomposites exhibits improved properties. The study proves through experimental studies that the materials produced have hexagonal wurtzite structures and enhanced optical property due to silver incorporation. Electrochemical performances of the materials demonstrate excellent capacitive performance, with up to 94% of retained capacitance after 10,000 cycles.

Dwivedi et al. [17] explores about the study on polyphenols extracted from plants as reducing and stabilizing agents in nanocomposite synthesis. Structural and morphological validation through XRD, SEM-EDS, and FTIR indicated successful structural incorporation and formation of the material. Efficacy of this compound in inhibiting Staphylococcus aureus and Candida albicans was confirmed. However, its low efficacy in inhibiting resistant bacteria requires additional improvement and study.

Krishnan et al. [18] studies on the antibacterial and antioxidative activity of derived bimetallic nanoparticles have been conducted by analyzing the synergistic effects on metal oxide interaction. The experiment utilizes state-of-the-art nanoparticle synthesis and characterization methods, including transmission electron microscopy, Fourier transform infrared spectroscopy, and X-ray diffraction. The results show efficient free-radical scavenging and antimicrobial activities. However, issues of scale-up, reproducibility, and stability require additional studies for real-world application.

Table.1 Summary on literature Review

Author	Key Contribution	Advantages	Disadvantages
Pratap et al. [11]	ZnO-MWCNT nanocomposites via sol-gel for energy storage	Improved dielectric constant and conductivity	Lacks stability and device integration
Kumari et al. [12]	Zn-doped nickel chromites for multifunctional use	Better bioactivity and magnetic properties	Limited biocompatibility validation
Awad et al. [13]	Green synthesis of Ag-doped nanowires	Reduced bandgap and improved capacitance	Scalability and stability issues
Ekwujuru et al. [14]	CdS nanoparticles for antimicrobial activity	Effective against E. coli	Toxicity concerns
Zulfiqar et al. [15]	Green nanocomposites for antibiotic degradation	High photocatalytic efficiency	Limited real-world application
Raza et al. [16]	Ag@ZnO nanocomposites for supercapacitors	High capacitance retention	Device integration challenges
Dwivedi et al. [17]	Plant-based nanocomposites for antimicrobial use	Eco-friendly and effective	Weak against resistant strains
Krishnan et al. [18]	Bimetallic nanoparticles for antimicrobial and antioxidant activity	Strong activity and environmental potential	Scalability and stability issues

Table.1 demonstrates some of the major breakthroughs in the synthesis of nanocomposites for energy storage, antimicrobial, and environmental applications. The use of green synthesis techniques through the use of natural extracts has also proved to be more sustainable and functional. Nonetheless, there are some shortcomings associated with these developments, such as poor scalability, stability, and in-device operation capability. Furthermore, toxicity and inefficiency towards resistant microorganisms pose serious threats to future applications. Insufficient biocompatibility testing also poses a challenge.

2.1 Research gap

Despite several achievements made in green chemistry and nanomaterials with multifunctional characteristics, available research demonstrates that optimization of structure, electrochemistry, and antibacterial performance of the same systems is still lacking [19]. This is evident from the fact that most studies do not provide proper methods to validate their results with respect to comparable studies in this domain. Furthermore, issues related to stability and toxicity of nanomaterials and integrating them into working devices are not adequately addressed [20]. Energy-related applications and biomedical purposes form the primary scope of these studies, and scalability and application in real environments receive little attention. The current research will address the aforementioned deficiencies.

ISSN: 2096-3246
Volume 58, Issue 01, 2026

3. Methodology

Methodology applied in this research work was such that the aim was to formulate and characterize a functional nanomaterial by means of green synthesis. First of all, appropriate precursors along with natural reducing agents were selected to prepare the nanomaterials. After synthesis, purification, drying, and other related processes, various analyses were performed on the samples prepared. These included analysis with respect to structural, optical, morphology, elemental composition, and dielectric properties of the samples prepared. XRD, FTIR, UV-Vis, Raman, SEM, and EDX techniques were used for the above analyses. Besides, tests to measure electrical response at various frequencies were also performed by means of dielectric analysis. Moreover, biological activity was checked by performing antimicrobial and antifungal tests.

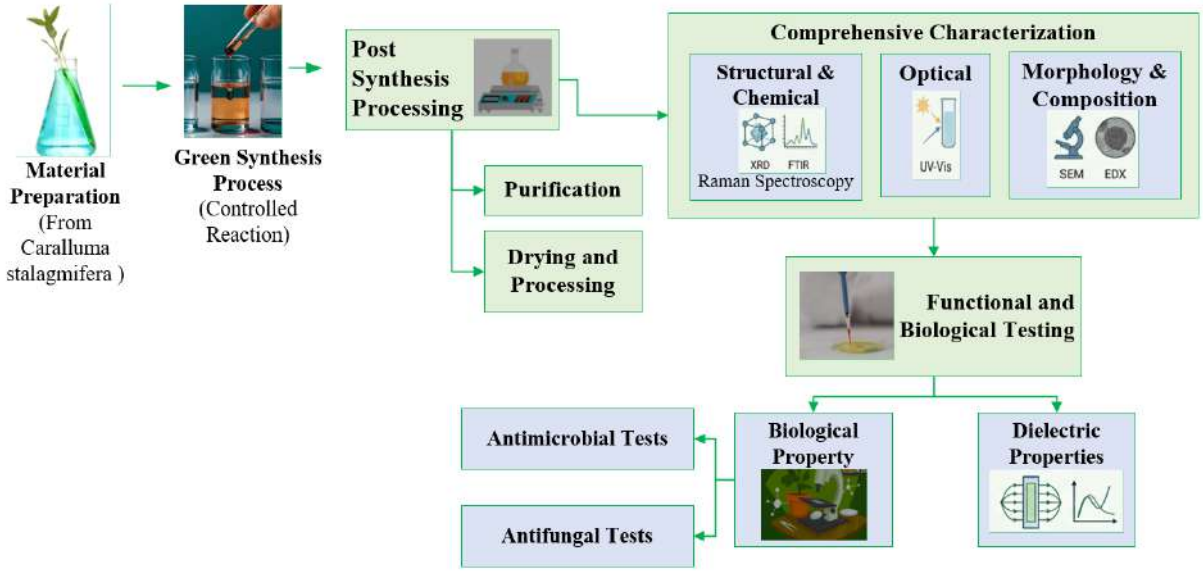

Fig.1 Methodology Flow diagram

Fig.1 presents the schematic flow chart used in the design of the total scheme that was applied in the green synthesis and investigation of the nanomaterial generated from the extract of *Caralluma stalagmifera*. First of all, the initial raw plant materials were collected and used in the synthesis of a green nanomaterial followed by its post-synthesis treatment. Next, the resultant product underwent purification, drying, and powdering to produce the stable nanostructure of the substance. Then, extensive characterization of the sample was done to characterize its structure, chemistry, optics, morphology, and composition using XRD, FTIR, Raman, UV-Vis, SEM, and EDX methods. Lastly, functional investigation was made to explore the functionality of the synthesized nanomaterial.

3.1 Materials

The materials required for the synthesis of the nanostructured samples were selected based on their purity and suitability for green synthesis. Analytical grade metal precursor salts containing sodium, potassium, cobalt, chloride, and silver sources were obtained from reliable commercial suppliers and used as received without further purification. Fresh *Caralluma stalagmifera* plant material was

collected from its natural habitat and utilized for the preparation of plant extract. Deionized water was used throughout the study for solution preparation, synthesis, and washing processes.

3.2 Preparation of Plant Extract

Fresh *Caralluma stalagmifera* plant material was harvested and rinsed several times using distilled water in order to eliminate adhering dust particles, dirt, and other contaminants. The rinsed plant material was placed in the shade and left to air dry for several days. Once the plant materials had been dried, they were minced to form powders with the help of an electric grinder. The plant material powders were then stored in airtight glass bottles. The steps of cleaning and drying were necessary to ensure that the powders had no contaminants and contained phytochemicals with reducing properties. This would make grinding and subsequent extraction processes easier.

The extraction process started by putting 10 g of the dried plant powder into a beaker containing 100 mL of distilled water. The solution was stirred for 30 minutes in a medium-heated condition using a magnetic stirrer to enable phytochemicals to diffuse from the plant powder into the water solution. When the heat was turned off, the solution was left to cool before filtration through Whatman No. 1 filter paper. The solution had a unique color which signified successful extraction of phytochemicals from the plant. The resulting plant extract was then stored under cold conditions awaiting nanoparticle synthesis.

3.3 Green Synthesis of Nanomaterial

The aqueous precursor solution was prepared using the appropriate number of salts of sodium, potassium, cobalt, chloride, and silver sources dissolved in distilled water as per the appropriate stoichiometry. This precursor solution was continuously stirred to ensure uniformity in the mixture. Subsequently, the recently prepared plant extract of *Caralluma stalagmifera* was introduced to the solution drop by drop in the presence of magnetic stirring. The controlled addition of plant extract assisted in controlling the nucleation and growth of nanoparticles. In order to reduce the metal ions, present in the solution, the solution was held at an appropriate temperature for a certain period of time. It should be highlighted that there was observed a color change in the reaction mixture, which indicated the start of the process of forming nanoparticles.

Once the reaction took place, the resulting precipitate was isolated by means of centrifugation and removed from the reaction mixture. The resulting precipitate was then washed with distilled water and ethanol to get rid of any unreacted precursors, organic matter, and any other contaminations. The purified precipitate was later dried using hot air oven at a proper temperature until all moisture was removed from the precipitate. The resulting dry precipitate was then finely ground into powder form using mortar and pestle. Two types of powders were produced through varying the ratios of precursors used. These powders were kept in sealed containers for analysis purposes. It can be stated that this method of synthesizing resulted in a green synthesis technique.

3.4 Characterization Techniques

Advanced methods for characterization were adopted in the investigation of the physicochemical properties of the produced nanomaterials. The structural characterizations were undertaken to establish the crystalline phase, the lattice system, and the purity of the material. The spectroscopy methods were employed for determining the chemical bonding, functional group, and optical

absorption characteristics. Morphological characterization entailed the investigations carried out on particle shapes, crystal structure, and surface morphology. Elemental analysis was done to confirm the elements in the synthesized material. Dielectric characterizations entailed the investigations done to find out electrical properties at various frequencies.

3.4.1 Diffraction

The structure, phase formation, and purity of the synthesized nanomaterials were studied using XRD method within a specific range of scanning angle of diffraction (2θ). The peaks acquired from the diffractogram were matched against reference patterns to find out the crystalline phase and synthesis of the required nanomaterials. Sharp and clear peaks in the diffractogram indicated that the samples were highly crystalline; meanwhile, lack of additional peaks indicated that there were no impurities in the synthesized phase. Peak intensity and width were changed to analyze the effect of composition on crystal growth and structural arrangement. Distance between the planes for the peaks was found out according to Bragg's equation. Average crystallite sizes of the synthesized samples were calculated according to the Debye-Scherrer equation considering the peak of maximum intensity in the diffractogram. Using Bragg's law, the interplanar spacing was determined as given in Eq. (1),

$$n\lambda = 2d\sin\ \theta \tag{1}$$

Where n is the diffraction order, λ is the wavelength of incident X-ray radiation, d is the interplanar spacing, and θ is the Bragg diffraction angle. The mathematical expression for Debye–Scherrer is given in Eq. (2),

$$D = \frac{K\lambda}{\beta\cos\ \theta} \tag{2}$$

Where D is the crystallite size, K is the shape factor, λ is the X-ray wavelength, β is the full width at half maximum FWHM of the diffraction peak, and θ is the Bragg angle.

3.4.2 UV–Visible Spectroscopy

Optical absorption characteristics of the synthesized nanomaterials were analyzed by means of UV-Visible Spectroscopy in the wavelength range of 200 to 800 nm. The measured optical absorption spectrum was then used to evaluate the interaction between the incident light and the synthesized nanomaterials, as well as their optical behavior. Since there were specific absorption thresholds and peaks in the optical absorption spectrum, it suggested that electronic excitations occurred inside the synthesized nanomaterials. Variations in the absorption intensities and absorption peaks were used to evaluate the influence of particle sizes, crystal structures, and compositions on the optical properties of the nanomaterials. The wavelength corresponding to the highest light absorption was used to provide relevant information regarding the ability of light absorption of the synthesized nanomaterials. In addition, the optical band gap energies of the samples were determined using the Tauc relation derived from the absorption spectrum. The absorption coefficient was determined using the Eq. (3)

$$\alpha = \frac{2.303A}{t} \tag{3}$$

Where α is the absorption coefficient, A is the measured absorbance, and t is the thickness of the sample.

The optical band gap energy was calculated using the Tauc equation Eq. (4)

$$(\alpha h\nu)^n = A(h\nu - E_g) \quad (4)$$

Where α is the absorption coefficient, $h\nu$ is the photon energy, A is a constant, Eg is the optical band gap energy, and n depends on the type of electronic transition.

The UV-visible spectrometry gave vital data about light absorbing properties as well as electron transitions of the nanomaterial formed. The calculated energy band gap helped understand its semiconductor properties as well as how suitable it is for future usage. Differences in optical properties were related to changes in composition and size of the particles. Hence, UV-visible spectrometry was crucial for assessing the photonic properties of the materials.

3.4.3 FTIR

The FTIR spectroscopic analysis was performed to identify the functional groups and chemical bonds existing in the prepared nanomaterial. For this purpose, the spectra were collected in the wavenumber range of 4000-400 cm-1 which includes the typical vibrations corresponding to the common organic and inorganic functional groups. Based on the results, various vibrations such as those corresponding to hydroxyl, carbonyl, amine, alkane, and metal-oxygen functional groups were identified in the prepared nanoparticles using FTIR. Changes in peak location and band intensities also indicated that there was interaction between plant phytochemicals and metal ions in the process of nanoparticle preparation. The FTIR analysis also aided in establishing the significance of plant extract in the reduction and stabilization of metal ions. The identification of metal-oxygen vibrations at lower wavenumbers showed that the formation of nanostructured material was successful. Therefore, FTIR analysis became a useful technique for characterizing the chemical nature and bonding of the prepared material. The transmittance of infrared radiation through the sample can be related in Eq. (5)

$$T = \frac{I}{I_0} \quad (5)$$

Where T is transmittance, I is the transmitted intensity, and I_0 is the incident infrared intensity. The absorbance was determined using the Beer–Lambert Eq. (6)

$$A = \log\left(\frac{I_0}{I}\right) \quad (6)$$

Where A is absorbance, I_0 is the incident intensity, and I is the transmitted intensity. The spectra acquired revealed the involvement of phytochemicals as well as metal-ligand complexation during the synthesis process. The FTIR test results also confirmed the formation of metal-oxygen bonds as well as capping of the synthesized nanoparticles.

3.4.4 Raman Spectroscopy

Raman spectroscopic analysis was performed to determine the vibrational properties, chemical bonding, and structural defects that may exist in the nanomaterials. The obtained Raman spectra helped in acquiring vital information about molecular bonding and vibration of the prepared material. Changes in position and peak intensity helped us understand the effect of composition on the structure of the prepared compound. The detection of characteristic Raman peaks helped ascertain that the prepared nanostructure had indeed been synthesized. Peak broadening and peak shifting also indicated the nanoscale effect and presence of defects in the prepared materials. Thus, Raman

spectroscopy was found to be an effective technique for analyzing the structural properties of the material.

3.4.5 Scanning Electron Microscopy

Using SEM, Observations on the morphology, surface, and particle size of the nanomaterial were investigated. Observations made by SEM indicated the following characteristics of the synthesized nanomaterials, such as its shape, surface, and particle size. Pictures taken by SEM were examined under various magnifications to analyze the presence of nanoparticles within the surface of the material. One phenomenon responsible for determining the characteristics of the nanoparticles was their agglomeration. Grain structures were also studied to assess how synthesis parameters affected the growth of grains. Thus, SEM was crucial for analyzing the morphology and surface quality of the produced nanomaterial.

3.4.6 Energy Dispersive X-ray Spectroscopy

The study of EDX, in conjunction with SEM, was carried out in order to ascertain the element compositions and purity levels of the nanomaterials developed. According to the results of the energy dispersive x-ray analysis of the samples, there was an indication that there were several elements present in the sample material. Some of the elements included oxygen, sodium, chlorine, potassium, cobalt, and silver. Weight percentage and atomic percentage of each of the elements were obtained during the quantitative analyses process. Relative intensity of each element's peaks also gave insight into their presence and distribution within the material. There was also lack of impurities within the sample.

3.4.7 Dielectric Measurements

Dielectric characteristics of the fabricated nanomaterial were evaluated using pelletized samples at specific frequencies at room temperature. In this regard, the powdered materials were pressed into circular pellets of constant thickness utilizing a hydraulic press. Conductive substances were applied to both sides of the pellets to achieve reliable electrical connection during testing. The dielectric characteristics of the samples were tested by subjecting them to an alternating electric field at various frequencies. Frequency-dependent changes in dielectric constant were studied to identify the physical phenomena responsible for polarization inside the sample. Dielectric loss was recorded to determine the extent of energy loss due to charge carrier mobility and dipole reorientation. Values of tangent loss were also calculated to quantify the insulation effectiveness of the fabricated samples. The dielectric constant was calculated using the Eq.7,

$$\varepsilon_r = \frac{Cd}{\varepsilon_0 A} \tag{7}$$

Where εr is the dielectric constant, C is capacitance, d is pellet thickness, ε_0 is the permittivity of free space, and A is the cross-sectional area of the pellet. The tangent loss was determined using the Eq. (8)

$$\tan\ \delta = \frac{\varepsilon''}{\varepsilon'} \tag{8}$$

Where *tan* δ is the loss tangent, ε'' is dielectric loss, and ε' is dielectric constant.

3.5 Antimicrobial and Antifungal Activity

The biological efficiency of the synthesized nanomaterials was tested by the means of antimicrobial and antifungal tests with the help of agar diffusion. Agar plates were inoculated with chosen bacterial and fungi cultures, and then holes were made for adding the synthesized materials in the form of suspension. After some incubation periods at appropriate temperature, inhibition zones were observed due to suppressed microbial growth. These inhibitions zones were measured in terms of their diameters to understand the performance of synthesized samples. Comparative analysis among different compositions was made to find out the most efficient material biologically. So, these experiments proved that the synthesized nanomaterial could be used for antimicrobial and antifungal purposes. All tests were repeated three times, and their results were reported in terms of mean ± standard deviation.

4. Results and Discussion

The Section outlines the results generated from the extensive study of the characterized and evaluated synthesized nanomaterials in terms of structure, performance, and their applications. Structural characteristics were assessed using XRD technique for the determination of crystalline phase and purity of the material. FTIR, UV-Visible, and Raman spectral techniques were applied for the study of chemical bonds, optical properties, and vibration characteristics of the sample. Surface morphology and size distribution of the particles were measured using SEM. Composition of the synthesized material was identified using EDX technique. Moreover, dielectric studies were conducted in order to study the electrical behavior at various frequencies. Antimicrobial and antifungal activities were determined for the assessment of biological properties of the synthesized material. The obtained results are discussed in detail and relationships between the characteristics of the material were established.

4.1 Multimodal Spectroscopic Evaluation

Different types of spectroscopy studies were done to evaluate the structure, chemistry, and optics of the synthesized nanomaterial in detail. XRD, FTIR, UV-Vis, and Raman spectroscopic analyses were used for gaining insights on crystallinity, bonding, absorbance, and vibrations. Such analytical tools were helpful in understanding the effects of green synthesis on the material preparation process. Changes observed in the spectra revealed the impact of composition on the materials synthesized. Thus, the multimodal spectroscopic study proved that the synthesized nanomaterial was successfully made.

ISSN: 2096-3246
Volume 58, Issue 01, 2026

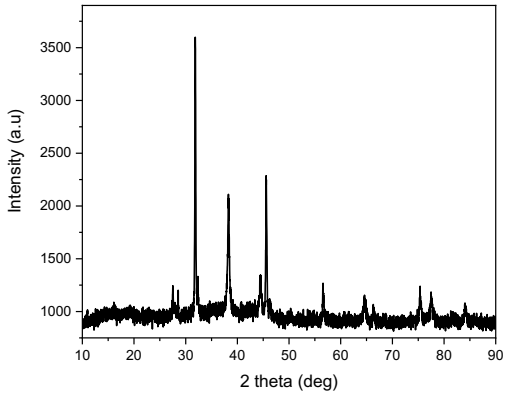

Fig.2 XRD Analysis

Fig.2 shows the XRD analysis. The XRD spectrum of the obtained nanomaterial contains sharp and well-defined diffraction peaks, which proves that the synthesized nanomaterial is crystalline. Intense peaks at particular 2θ values signify the successful formation of the phase with high crystallinity and purity. The broadening of peaks at some regions implies the formation of nanocrystals within the material. The analysis of the XRD data shows that the synthesis of the nanostructured sample was performed successfully.

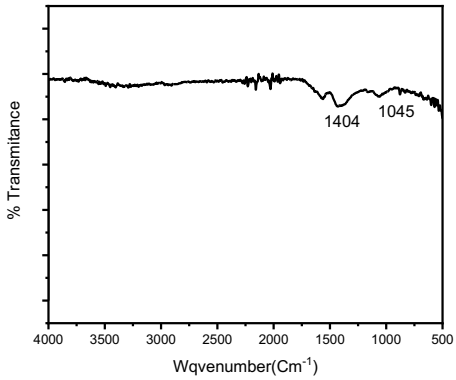

Fig.3 FTIR Analysis

From the Fig.3, it is evident that there are some characteristic bands, which show that there are functional groups in the nanomaterials that have played a significant role in their production and stabilization. The strong peaks in the graphs at about 1404 cm^{-1} and 1045 cm^{-1} can be said to correspond to the bending and stretching vibrations of bonds present in the organic materials and metal-oxygen compounds.

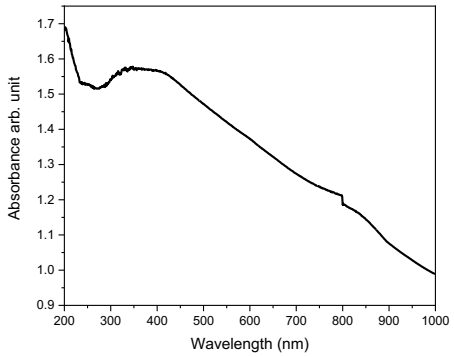

Fig.4 UV–Visible Analysis

Fig.4 shows strong absorbance at low wavelengths. This clearly indicates effective absorption by the material upon interaction with the light source. Absorbance gradually decreases with an increase in wavelength. This may be due to semiconductor-like properties of the material under investigation. The estimated energy bandgap of the material is indicative of its applicability for use in optoelectronics and photo catalysis.

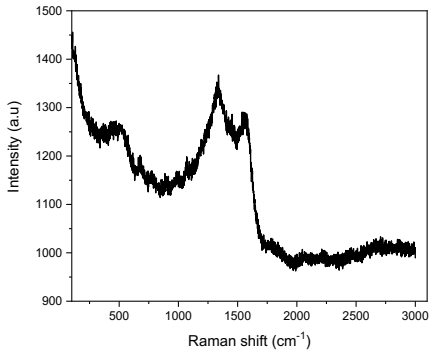

Fig.5 Raman Analysis

Fig.5 shows the Raman analysis. The vibration pattern of the engineered Cu bimetallic nanoparticles is clearly seen in their Raman spectra. The major peaks found in the region between 1200 and 1600 cm^{-1} indicate the presence of vibrations that belong to metal-oxygen bonds, along with some other vibrations due to organic functional groups arising from the plant compounds. The broadening and intensity changes further confirm the stabilizing role of the phyto-compounds on the nanoparticle surface. In addition, the low intensity beyond 1800 cm^{-1} reveals very few structural flaws, proving the creation of highly stabilized bimetallic nanoparticles.

4.2 Morphological Evaluation

Morphological studies were conducted to study the morphology of the material at the nanoscale level, including the investigation of surface morphology, particle distribution, and homogeneity of the structures produced. SEM and EDX have been used for detailed investigations of particle morphology, agglomeration tendencies, grain boundary structure, and elemental analysis. Such studies were useful for understanding the effects of the green method of nanomaterial preparation on

surface morphology. The obtained surface characteristics are essential for determining the optical, electrical, and biological activity of the obtained samples.

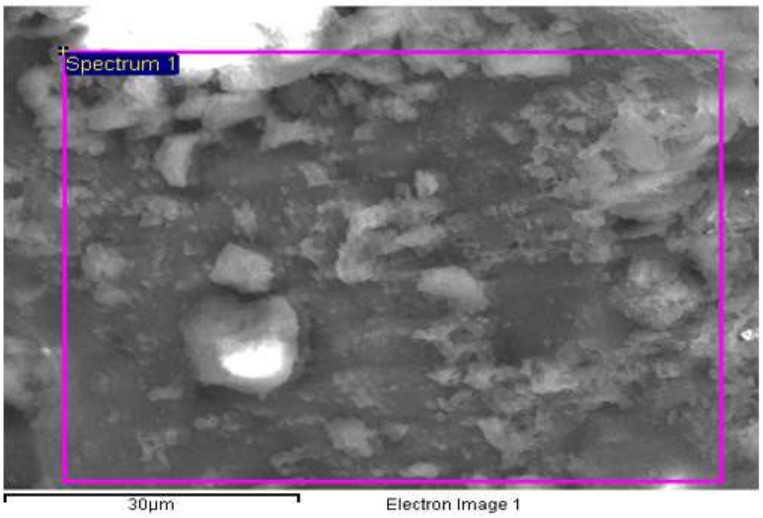

Fig.6 SEM Analysis

Fig.6 shows the SEM image of the phyto-synthesized bimetallic nanoparticles demonstrates that the morphology is irregular and agglomerated with uneven distribution of nanoparticles. The presence of clustered nanoparticles shows that there are strong interactions between the particles and efficient capping by biomolecules from the plants. The particles are in both granular and flake form, which shows that nucleation occurs heterogeneously during synthesis.

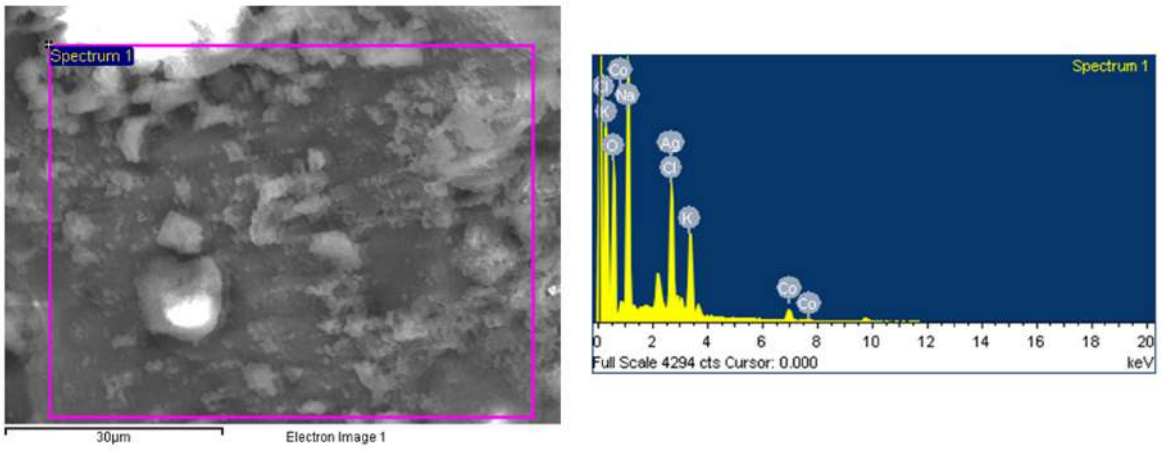

Fig.7 EDX Analysis

Fig.7 shows the EDX analysis. The elemental makeup is also validated by the EDX spectrum of the Cu-based bimetallic phyto-engineered nanostructures in terms of the presence of sharp Cu peaks together with peaks for the secondary metal components. Peaks for oxygen (O), which denote possible partial oxidation or metal oxide formations, and peaks for carbon (C), which come from

phytochemicals present as stabilizing capping agents, have also been observed in the spectrum. Other trace elemental peaks may be due to the presence of biomolecules or instrument artifacts.

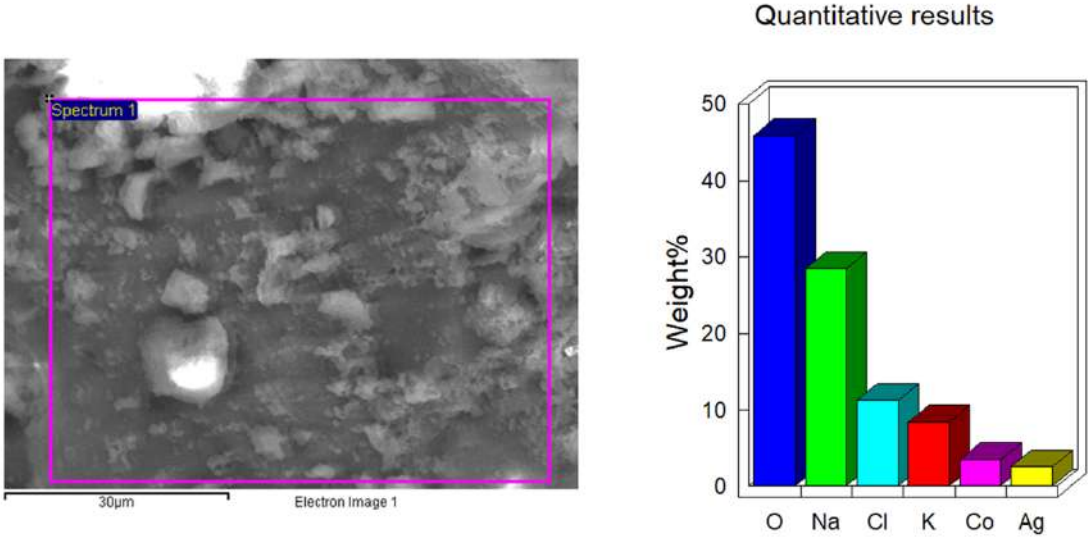

Fig.8 EDX Quantitative Material

According to the Fig.8, the elements present are primarily oxygen (O), implying that oxides have been formed and are providing stability on the surface. The contributions made by sodium (Na) and chlorine (Cl) are also prominent, meaning that the biomaterials from plants and precursors have remained on the surface. Trace amounts of potassium (K), cobalt (Co), and silver (Ag) imply that other metals apart from copper have been incorporated into the nanoparticles.

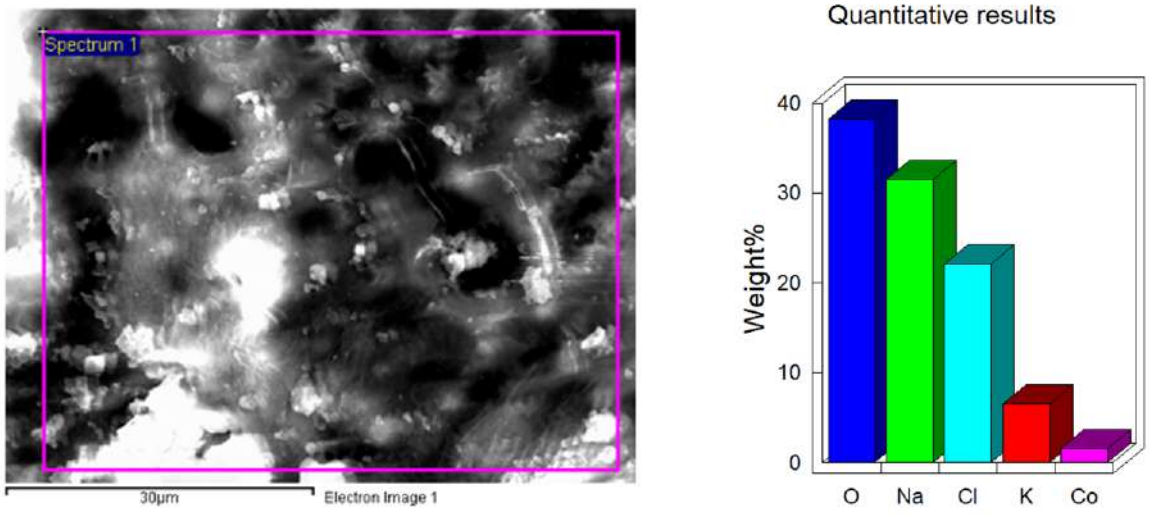

Fig.9 SEM and EDX analysis

As seen from the Fig.9, there is an irregular agglomeration of particles with non-uniform distribution in shape, which implies that there are strong particle interactions during the synthesis process. There exist cluster formations and flake-like structures in the image, showing heterogenous nucleation and

stabilization through plant extracts. As can be deduced from the EDX quantification, oxygen is the major component followed by sodium and chlorine. Potassium and cobalt are the minor components.

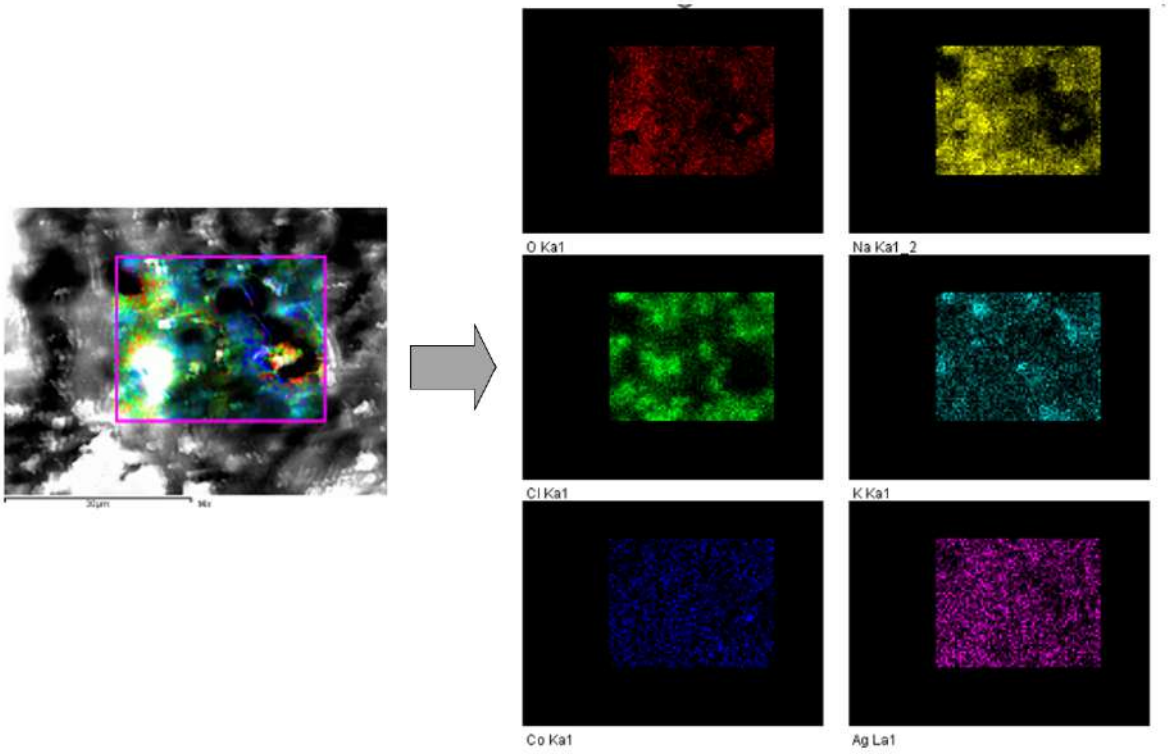

Fig.10 SEM image with elemental mapping

Fig.10 illustrates the spatial distribution of these elements on the nanostructure that has been formed, thus proving the successful incorporation of multiple elements. The element oxygen has a highly concentrated distribution pattern which means that oxides have been successfully formed during this process. Elements such as sodium and chlorine have a relatively evenly distributed concentration, showing that they have been incorporated from the precursors and plants used. Potassium and cobalt also have fairly concentrated spatial distribution, proving that they have been used as second elements in this composition.

4.3 Functional Performance Evaluation

Performance evaluation in terms of functionality was performed to investigate the practical utility and multi-functional nature of the fabricated nanostructure. Electrical properties and effectiveness against microorganisms were investigated using dielectric, antimicrobial, and antifungal studies. Information about the effectiveness of the nanomaterial in terms of frequency-dependent behavior, effectiveness against microorganisms, and stability was obtained through this testing process. Performance was found to be highly dependent upon the composition, surface nature, and structure at the nanoscale level of the synthesized nanostructure.

ISSN: 2096-3246
Volume 58, Issue 01, 2026

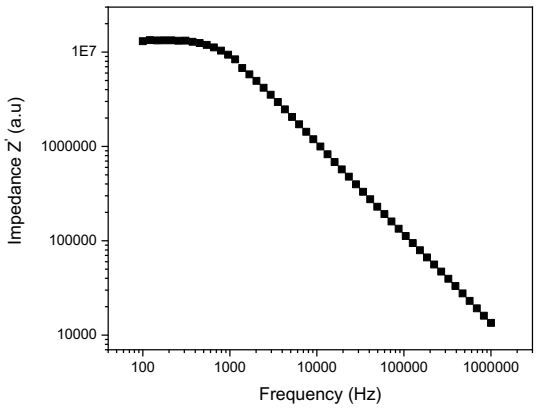

Fig.11 Dielectric (Frequency Vs Independence)

According to Fig.11, the impedance value (Z) decreases with an increase in the frequency value, suggesting that there is better electrical conductivity as the frequency value becomes greater. The impedance values being very high at lower frequencies are due to the effects of charge transfer resistance and polarization of the electrodes.

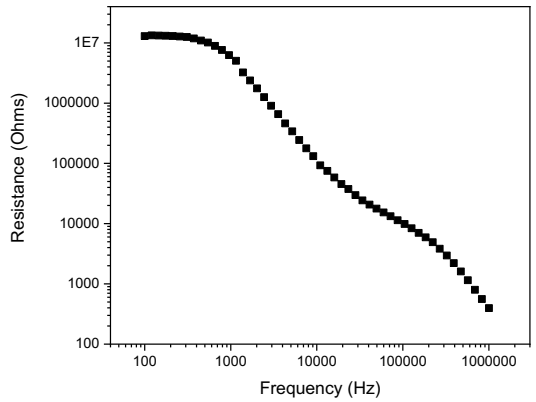

Fig.12 Dielectric (Frequency Vs Resistance)

It can be seen from the Fig.12, that the resistance decreases with an increase in frequency, suggesting better charge mobility at a higher frequency. The presence of high resistance at low frequencies could be attributed to the effect of grain boundaries and limited motion of charges. When the frequency is increased, the charge carriers acquire enough energy to jump from one state to another, causing a sudden decrease in resistance.

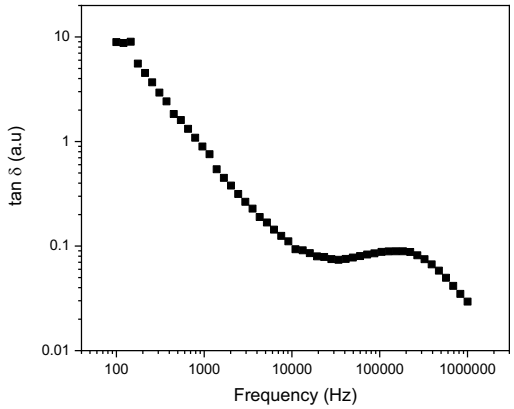

Fig.13 Variation of dielectric loss tangent

Fig.13 shows significant reduction with an increase in frequency, which implies that lesser energy is lost with a rise in frequency. The loss tangent of high value at low frequencies could be due to the formation of space charges and their accumulation at grain boundaries. As the frequency rises, the dipolar polarization will not be able to accept with changes in the rapidly varying electric field, and hence losses will become less.

Fig.14 Antimicrobial activity

Fig.14 shows the antimicrobial properties of the produced nanoparticles, that were assessed using the agar well diffusion technique; the zones of inhibition were clearly observable around the nanoparticles. Concentration-dependent antimicrobial activity of the nanoparticles was observed from the different size inhibition zones obtained for the nanoparticles on various plates. The produced nanoparticles displayed significant antimicrobial properties, implying that they have good biocidal properties. Their increased efficacy is due to the combination of metal ions and phytochemicals.

Table.2 Antifungal activity

7.1±0.5		3.7±0.9		2.5±0.69	

Table.2 shows the antifungal activity. The results showed that the zone of inhibition recorded were 7.1 ± 0.5mm, 3.7± 0.9 mm, and 2.5 ± 0.69 mm, showing that there was a difference in the level of efficiency in terms of antifungal activity. The largest zone of inhibition indicates that the antimicrobial is more efficient at a high concentration or effective against a particular microorganism.

4.4 Discussion

The results show that the fabrication of bimetallic nanoparticles through phytoengineering is successfully achieved by obtaining the required enhanced multifunctionality. Crystalline nature and phase purity are confirmed by XRD, whereas the presence of phytochemicals in the process is evidenced by FTIR and Raman spectroscopy through interactions between the metals and oxygen-containing moieties, as well as organic functional groups. The results of UV–Visible analysis suggest high absorbance with semiconducting properties, making such nanomaterial useful for optoelectronic applications. Through SEM and EDX analysis along with elemental mapping, agglomeration and proper distribution of bimetallic nanoparticles with elemental composition can be confirmed.

5. Conclusion and Future works

A functional nanomaterial was effectively synthesized via a green synthesis approach with the aid of a natural plant extract, acting as a reducing and stabilizing agent. Extensive characterization, conducted via Multimodal Spectroscopic Evaluation and dielectric analysis, ensured the structural confirmation, functional groups, optical behavior, surface morphology, chemical composition, and electrical properties of the synthesized nanoparticles. The results indicated promising structural stability, optical behavior, and functional effectiveness of the prepared material. In addition, studies on antimicrobial and antifungal properties showed the biological efficiency of the synthesized material against selected pathogenic species. Thus, the synthesized nanomaterial shows considerable potential in the field of sensing, biomedical coatings, environmental treatment, and electronic devices.

In future research, the synthesis conditions could be fine-tuned to manipulate the size, shape, and composition of the material. Future studies on photo-catalysis, energy storage through electrochemistry, and sensing applications would help increase applications of the material. Additionally, biocompatibility testing should be done before employing the nanomaterial in biological processes. Further investigation into large-scale synthesis and stability could also be considered.

References

[1] M. Saeed, H. M. Marwani, U. Shahzad, A. M. Asiri, and M. M. Rahman, “Recent Advances, Challenges, and Future Perspectives of ZnO Nanostructure Materials Towards Energy Applications,” *The Chemical Record*, vol. 24, no. 1, p. e202300106, Jan. 2024, doi: 10.1002/tcr.202300106.

[2] S. Raha and Md. Ahmaruzzaman, “ZnO nanostructured materials and their potential applications: progress, challenges and perspectives,” *Nanoscale Adv.*, vol. 4, no. 8, pp. 1868–1925, 2022, doi: 10.1039/D1NA00880C.

[3] N. Joudeh and D. Linke, “Nanoparticle classification, physicochemical properties, characterization, and applications: a comprehensive review for biologists,” *J Nanobiotechnol*, vol. 20, no. 1, p. 262, Jun. 2022, doi: 10.1186/s12951-022-01477-8.
[4] M. F. Acosta HumÃ¡nez *et al.*, “An overview of Basic Characterization Techniques for Natural originated Biopolymers: UV-Vis and FTIR spectroscopy- A review,” *J. Sci. Technol. Appl.*, vol. 18, pp. 1–9, May 2025, doi: 10.34294/j.jsta.25.18.106.
[5] S. Thakur *et al.*, “Graphene oxide as smart sustainable nanomaterial: a versatile multifunctional material with transformative potential in advanced materials science research,” *npj Mater. Sustain.*, vol. 4, no. 1, p. 8, Mar. 2026, doi: 10.1038/s44296-026-00095-x.
[6] K. Hachem *et al.*, “Methods of Chemical Synthesis in the Synthesis of Nanomaterial and Nanoparticles by the Chemical Deposition Method: A Review,” *BioNanoSci.*, vol. 12, no. 3, pp. 1032–1057, Sep. 2022, doi: 10.1007/s12668-022-00996-w.
[7] M. A. Sebak, T. F. Qahtan, G. M. Asnag, and E. M. Abdallah, “The Role of TiO2 Nanoparticles in the Structural, Thermal and Electrical Properties and Antibacterial Activity of PEO/PVP Blend for Energy Storage and Antimicrobial Application,” *J Inorg Organomet Polym*, vol. 32, no. 12, pp. 4715–4728, Dec. 2022, doi: 10.1007/s10904-022-02440-8.
[8] B. Mekuye and B. Abera, “Nanomaterials: An overview of synthesis, classification, characterization, and applications,” *Nano Select*, vol. 4, no. 8, pp. 486–501, Aug. 2023, doi: 10.1002/nano.202300038.
[9] N. Al-Harbi and N. K. Abd-Elrahman, “Physical methods for preparation of nanomaterials, their characterization and applications: a review,” *J.Umm Al-Qura Univ. Appll. Sci.*, vol. 11, no. 2, pp. 356–377, Jun. 2025, doi: 10.1007/s43994-024-00165-7.
[10] R. Khan *et al.*, “Carrier-mediated ferromagnetism and dielectric tailoring in dual-doped ZnO semiconductor nanoparticles for spintronics,” *Materials Science in Semiconductor Processing*, vol. 193, p. 109487, Jul. 2025, doi: 10.1016/j.mssp.2025.109487.
[11] R. Pratap *et al.*, “Investigations on structural, microstructural, dielectric and electrical conductivity of the ZnO-MWCNTs nanocomposite synthesized via sol-gel method,” *Oxford Open Materials Science*, vol. 5, no. 1, p. itaf006, Jan. 2025, doi: 10.1093/oxfmat/itaf006.
[12] P. S. Kumari, N. Gadwala, and G. V. Charan, “Structural, magnetic, dielectric, and antimicrobial investigations of enhanced Zn-doped Ni nano chromites,” *Results in Chemistry*, vol. 18, p. 102729, Nov. 2025, doi: 10.1016/j.rechem.2025.102729.
[13] M. A. Awad, K. M. O. Ortashi, K. Alzahrani, and H. Althobaiti, “Solvothermal eco-synthesis of Ag-Doped ZnO nanowires: investigation of structural, optical, dielectric, and electrochemical properties,” *Journal of Taibah University for Science*, vol. 19, no. 1, p. 2552591, Dec. 2025, doi: 10.1080/16583655.2025.2552591.
[14] E. U. Ekwujuru, M. G. Peleyeju, C. Ssemakalu, M. Monapathi, and M. Klink, “Characterization and Antimicrobial Assessment of Cadmium Sulfide Nanoparticles,” *IJMS*, vol. 27, no. 1, p. 432, Dec. 2025, doi: 10.3390/ijms27010432.
[15] N. Zulfiqar, R. Nadeem, and O. A. Musaimi, “Photocatalytic Degradation of Antibiotics via Exploitation of a Magnetic Nanocomposite: A Green Nanotechnology Approach toward Drug-

Contaminated Wastewater Reclamation," *ACS Omega*, p. acsomega.3c08116, Feb. 2024, doi: 10.1021/acsomega.3c08116.

[16] A. Raza *et al.*, "Green Synthesis of ZnO Nanoparticles and Ag-Doped ZnO Nanocomposite Utilizing *Sansevieria trifasciata* for High-Performance Asymmetric Supercapacitors," *ACS Omega*, p. acsomega.3c10060, Jul. 2024, doi: 10.1021/acsomega.3c10060.

[17] P. Dwivedi *et al.*, "Plant-mediated synthesis, characterization, and evaluation of a copper oxide/silicon dioxide nanocomposite by an antimicrobial study," *Nanotechnology Reviews*, vol. 13, no. 1, p. 20240105, Oct. 2024, doi: 10.1515/ntrev-2024-0105.

[18] A. Krishnan *et al.*, "Metal oxides on the frontlines: Antimicrobial activity in plant-derived biometallic nanoparticles," *Nanotechnology Reviews*, vol. 13, no. 1, p. 20240106, Dec. 2024, doi: 10.1515/ntrev-2024-0106.

[19] M. K. Sah, B. S. Thakuri, J. Pant, R. L. Gardas, and A. Bhattarai, "The Multifaceted Perspective on the Role of Green Synthesis of Nanoparticles in Promoting a Sustainable Green Economy," *Sustainable Chemistry*, vol. 5, no. 2, pp. 40–59, Mar. 2024, doi: 10.3390/suschem5020004.

[20] S. M. Abegunde, M. O. Alaka, and O. I. Awonyemi, "Nanomaterial toxicity: a comprehensive review of mechanisms and mitigation strategies," *Discov. Hazards*, vol. 1, no. 1, p. 3, Nov. 2025, doi: 10.1007/s44475-025-00003-2.